PHYSICAL REVIEW B **93**, 020404(R) (2016)

Skyrmions in chiral magnets with Rashba and Dresselhaus spin-orbit coupling

James Rowland,[1] Sumilan Banerjee,[2] and Mohit Randeria[1]
[1]*Department of Physics, The Ohio State University, Columbus, Ohio 43210, USA*
[2]*Department of Condensed Matter Physics, Weizmann Institute of Science, Rehovot 7610001, Israel*
(Received 8 October 2015; published 19 January 2016)

Skyrmions are topological spin textures of interest for fundamental science and applications. Previous theoretical studies have usually focused on chiral magnets with broken bulk inversion symmetry, with skyrmions stabilized by easy-axis anisotropy. We investigate here systems that break surface inversion (mirror symmetry) in addition to bulk inversion. This leads to two distinct Dzyaloshinskii-Moriya (DM) terms with strengths $D_\perp$, arising from Rashba spin-orbit coupling (SOC), and $D_\parallel$ from Dresselhaus SOC. We show that skyrmions become progressively more stable with increasing $D_\perp/D_\parallel$ and extend into the regime of easy-plane anisotropy. We find that the spin texture and topological charge density of skyrmions develops a nontrivial spatial structure with quantized topological charge in a unit cell given by a Chern number. Our results give a design principle for tuning Rashba SOC and anisotropy to stabilize skyrmions in thin films, surfaces, interfaces, and bulk magnetic materials that break mirror symmetry.

DOI: 10.1103/PhysRevB.93.020404

Recently there has been a surge of interest in skyrmions in chiral magnetic materials [1–3], ranging from fundamental science to potential device applications. A skyrmion is a spin texture characterized by a topological invariant that gives rise to the topological Hall effect [4,5] and may also have implications for non-Fermi-liquid behavior [6]. The ability to write and erase individual skyrmions [7], along with their topological stability, small size, and low depinning current density [8], paves the way for potential information storage and processing applications.

Experiments have focused primarily on noncentrosymmetric crystals with broken bulk inversion symmetry: metals such as MnSi and FeGe and insulators such as Cu_2OSeO_3. In these materials, the skyrmion crystal (SkX) phase is stable only in a very limited region of the magnetic field (H), temperature (T) phase diagram [9–13]. On the other hand, the skyrmion phase is found to be stable over a much wider region of (T, H) in thin films of the same materials [10,14–16], even extending down to $T = 0$ in some cases [14,16].

A key question that we address in this Rapid Communication is as follows: How can we enhance the domain of stability of skyrmion spin textures? We are motivated in part by the thin film experiments, and also by the possibility of chiral magnetism in new two-dimensional (2D) systems such as oxide interfaces [17–19]. We show how the SkX becomes progressively more stable over ever larger regions in parameter space of field H and magnetic anisotropy A, as the effects of broken surface inversion dominate over those of broken bulk inversion.

We begin by summarizing our main results, which requires us to introduce some terminology. We focus on magnets in which spin textures arise from the interplay between ferromagnetic exchange J and the chiral Dzyaloshinskii-Moriya (DM) interaction $\mathbf{D}_{ij} \cdot (\mathbf{S}_i \times \mathbf{S}_j)$. Spin-orbit coupling (SOC) determines the magnitude of the $\mathbf{D}$ vector, while symmetry dictates its direction. Broken bulk inversion symmetry ($\mathbf{r} \to -\mathbf{r}$) leads to the Dresselhaus DM term with $\mathbf{D}_{ij} = D_\parallel\, \hat{\mathbf{r}}_{ij}$, where $\hat{\mathbf{r}}_{ij} = \mathbf{r}_{ij}/|\mathbf{r}_{ij}|$ with $\mathbf{r}_{ij} = (\mathbf{r}_i - \mathbf{r}_j)$. On the other hand, broken surface inversion or mirror symmetry ($z \to -z$) leads to the Rashba DM term with $\mathbf{D}_{ij} = D_\perp(\hat{\mathbf{z}} \times \hat{\mathbf{r}}_{ij})$. In the limit of weak SOC, $D/J \ll 1$, where $D = (D_\parallel^2 + D_\perp^2)^{1/2}$, the length scale of spin textures is $(J/D)a \gg a$ (the microscopic lattice spacing) and we can work with a continuum "Ginzburg-Landau" field theory [20].

We show in Fig. 1 the evolution of the $T = 0$ phase diagram going from the pure Dresselhaus limit to the pure Rashba limit. Each phase diagram is plotted as a function of the (dimensionless) field HJ/D^2 and anisotropy AJ/D^2. Here, $A > 0$ ($A < 0$) corresponds to easy-plane (easy-axis) anisotropy. Our main results are as follows:

(1) As the Rashba $D_\perp$ is increased relative to the Dresselhaus $D_\parallel$, the spiral and skyrmion phases become increasingly more stable relative to the vertical cone phase, and penetrate into the easy-plane anisotropy side of the phase diagram.

(2) With increasing $D_\perp/D_\parallel$, the textures change continuously from a Bloch-like spiral to a Néel-like spiral. Correspondingly, the skyrmion helicity evolves with a vortexlike structure in the Dresselhaus limit to a hedgehog in the Rashba limit, which is shown to impact the ferrotoroidic moment.

(3) In the pure Rashba limit, we find the largest domain of stability for the hexagonal skyrmion crystal. In addition, we also find a small sliver of stability for a square skyrmion lattice, together with an elliptic cone phase, distinct from the well-known vertical cone phase in the Dresselhaus limit.

(4) We see in Fig. 2 that in the Rashba limit the spin texture of the skyrmion and their topological charge density $\chi(\mathbf{r})$ begins to show nontrivial spatial variations as one changes anisotropy, but the total topological charge $N_{\rm sk} = \int d^2r\, \chi(\mathbf{r})$ in each unit cell remains quantized, even when $\chi(\mathbf{r})$ seems to "fractionalize" with positive and negative contributions within a unit cell.

(5) For $H > 2A$, one can have isolated skyrmions in a ferromagnetic (FM) background, and their topological charge $N_{\rm sk}$ is quantized, as usual, by the homotopy group $\pi_2(S^2) = \mathbb{Z}$. For $H < 2A$, we find that skyrmions cannot exist as isolated objects, and $N_{\rm sk}$ must now be defined by the $\mathbb{Z}$ Chern number classifying maps from the SkX unit cell, a two-torus T^2 to S^2, the unit sphere in spin space, a definition that works for all values of $H/2A$.

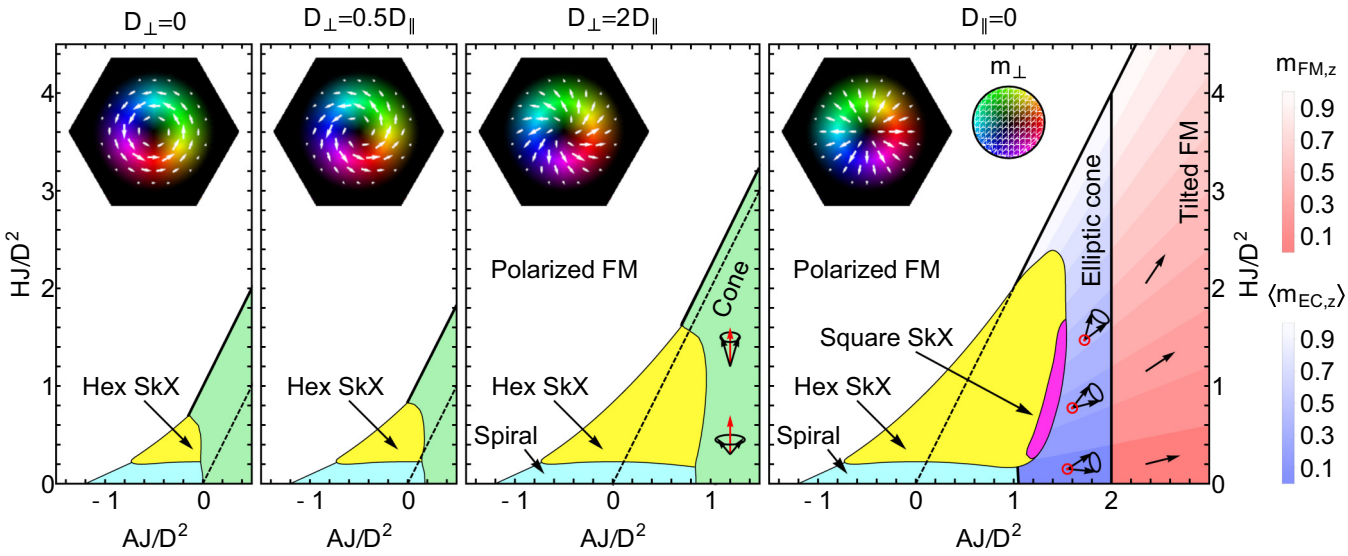

FIG. 1. Phase diagrams as a function of AJ/D^2 and HJ/D^2 for four values of $D_\perp/D_\parallel$. Easy-axis anisotropy corresponds to $A < 0$ while easy-plane anisotropy to $A > 0$. The cone, elliptic cone, and tilted FM phases are shown schematically, with the Q vector shown in red and the texture traced out by spins shown in black. The color bar on the right indicates m_z for the elliptic cone and tilted FM phases in the $D_\parallel = 0$ panel. Insets: Unit cell in the hexagonal (Hex) skyrmion crystal (SkX) phase with white arrows indicating the projection of magnetization on the x-y plane. The colors indicate the magnitude and direction of the spin projection following the convention of Ref. [3], indicated in the color wheel. Thick lines denote continuous transitions, while thin lines indicate first-order phase transitions.

Free energy. We consider a continuum (free) energy functional $F[\mathbf{m}] = \int d^3r \mathcal{F}(\mathbf{m})$ with

$$\mathcal{F} = \mathcal{F}_J + \mathcal{F}_{\rm DM} + \mathcal{F}_A - Hm_z, \qquad (1)$$

whose form is dictated by symmetry. The isotropic exchange term $\mathcal{F}_J = (J/2)\sum_\alpha (\nabla m_\alpha)^2$ $(\alpha = x,y,z)$ controls the gradient energy through stiffness J. The DM contribution in the

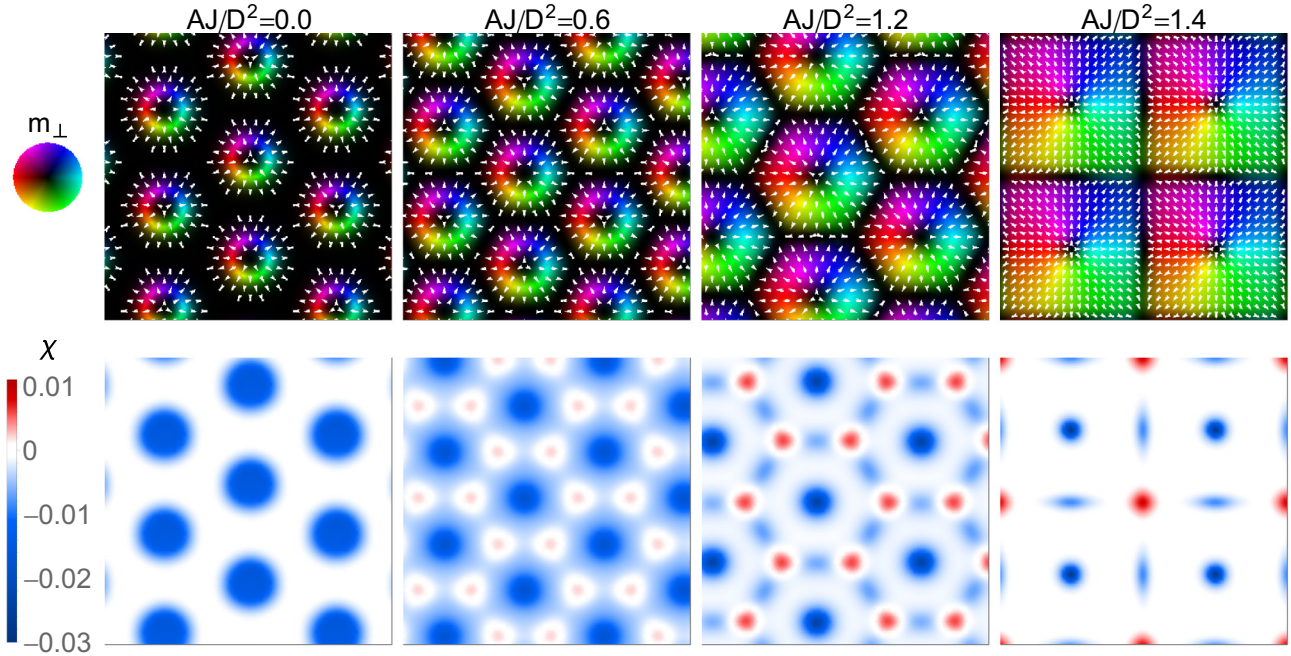

FIG. 2. Evolution of the spin texture $\mathbf{m}$ (top row) and the topological charge density χ (bottom row) for four values of AJ/D^2 at fixed $HJ/D^2 = 0.7$ in the Rashba limit ($D_\parallel = 0$). White arrows indicate the projection of $\mathbf{m}$ into the x-y plane. The colors also indicate the magnitude and direction of the spin projection following the convention of Ref. [3], indicated in the color wheel. The development of nontrivial spatial variation in $\chi(\mathbf{r})$ is discussed in the text. Note, however, that in each case the integral over a single unit cell, $\int d^2\mathbf{r}\,\chi(\mathbf{r}) = -1$.

continuum

$$\mathcal{F}_{\rm DM} = D\cos\beta\,\mathbf{m}\cdot(\nabla\times\mathbf{m}) + D\sin\beta\,\mathbf{m}\cdot[(\hat{\mathbf{z}}\times\nabla)\times\mathbf{m}] \tag{2}$$

is the sum of the two terms discussed above. The $D_\parallel = D\cos\beta$ term arises from Dresselhaus SOC in the absence of bulk inversion and $D_\perp = D\sin\beta$ from Rashba SOC with broken surface inversion. The anisotropy term $\mathcal{F}_A = Am_z^2$ can be either easy axis ($A<0$) or easy plane ($A>0$). Several different mechanisms contribute to A, including single-ion and dipolar shape anisotropies. In addition, Rashba SOC naturally leads to an easy-plane, compass anisotropy $A_\perp \simeq D_\perp^2/2J$, which is energetically comparable to the DM term [17,18,21,22]. We treat A as a free, phenomenological parameter.

We focus on $T=0$ where the local magnetization is constrained to have a fixed length $\mathbf{m}^2(\mathbf{r})=1$, and it should be hardest to stabilize skyrmions; once $|\mathbf{m}(\mathbf{r})|$ can become smaller due to thermal fluctuations, skyrmions should be easier to stabilize. It is convenient to scale all distances by the natural length scale J/D (setting the microscopic $a=1$) and scale the energy $\mathcal{F}$ by D^2/J. All our results will be presented in terms of the three dimensionless parameters that describe $\mathcal{F}$, namely, field HJ/D^2, anisotropy AJ/D^2, and $\tan\beta = D_\perp/D_\parallel$.

Our results are applicable for several distinct geometries. We implicitly apply periodic boundary conditions valid for (i) bulk materials and (ii) thin films [23] with thickness $\gg (J/D)a$. The results of the rightmost panel of Fig. 1 are also applicable to (iii) monolayer magnets. In films, we expect the Rashba $D_\perp$ and anisotropy A to depend on thickness and choice of substrate. While we expect Rashba SOC to be larger in thinner films, it can be substantial even in thick films due to strain gradients [24]. Quantitative estimates of the thickness and substrate dependence of these parameters require microscopic calculations beyond the scope of this Rapid Communication.

Phase diagram. In Fig. 1, we show the evolution of the (A,H) phase diagram as a function of $\tan\beta = D_\perp/D_\parallel$, increasing from left to right. These results were obtained by minimizing the energy functional $\mathcal{F}$ subject to $\mathbf{m}^2(\mathbf{r})=1$. The energies of the fully polarized ferromagnet (FM), tilted FM, and vertical cone states can be determined analytically, while the energies for the spiral, the skyrmion crystals, and the elliptic cone state were found by a numerical, conjugate gradient minimization approach. In all cases, the results were checked by semianalytical variational calculations. Details of the methodology are described in the Supplemental Material [25]; here, we focus on the results.

We begin with well-known [13] results in the Dresselhaus limit (left panel of Fig. 1), where the hexagonal SkX and spiral phases are stable only in a small region with easy-axis anisotropy ($A\leqslant 0$). The $A>0$ region is dominated by the vertical cone phase, where $\mathbf{m}_{\rm cone}(z) = [\cos\varphi(z)\sin\theta_0, \sin\varphi(z)\sin\theta_0, \cos\theta_0]$ with $\varphi(z) = D_\parallel z/J$ and $\cos\theta_0 = H/[2A + D_\parallel^2/J]$. The vertical cone-polarized FM phase boundary is given by $H = 2A + D_\parallel^2/J$.

We note a change of variables that greatly simplifies the analysis of skyrmion crystal and spiral phases. This transformation is useful when $\mathbf{m} = \mathbf{m}(x,y)$ has no z dependence (along the field). Using a rotation $R_z(-\beta)$ by an angle $-\beta$ about the z axis, we define $\mathbf{n}(x,y) = R_z(-\beta)\mathbf{m}(x,y)$. It is then easy to show that (2) simplifies to a pure Dresselhaus form $\mathcal{F}_{\rm DM} = D\mathbf{n}\cdot(\nabla\times\mathbf{n})$, while the other terms in (1) are invariant under $\mathbf{m}\to\mathbf{n}$.

We choose, without loss of generality, $\hat{\mathbf{x}}$ as the propagation direction for the spiral of period L, so that $\mathbf{n}_{\rm sp}(x) = [0, \sin\theta(x), \cos\theta(x)]$ with $\mathbf{n}_{\rm sp}(x+L) = \mathbf{n}_{\rm sp}(x)$. (Note that this is *not* in general a single-$\mathbf{q}$ spiral.) We minimize $\mathcal{F}$ to find the optimal L and optimal *function* $\theta(x)$, which is a one-dimensional (1D) minimization problem. For the SkX we pick a unit cell (hexagonal or square) and find its optimal size and optimal texture $\mathbf{n} = (\cos\varphi\sin\theta, \sin\varphi\sin\theta, \cos\theta)$, by solving a 2D minimization problem. We determine $\varphi(x,y)$ and $\theta(x,y)$ within a unit cell subject to periodic boundary conditions.

With increasing $D_\perp/D_\parallel$, we see that the SkX and spiral phases become more stable relative to the vertical cone, and their region of stability extends into the easy-plane regime. To understand this, consider increasing the Rashba $D_\perp$ keeping $D_\parallel$ fixed. The energy of cone $\mathbf{m}(z)$ depends only on $D_\parallel$, and is unchanged as $D_\perp$ increases. In contrast, the SkX and spiral, with $\mathbf{m} = \mathbf{m}(x,y)$, utilize the full $D = (D_\parallel^2 + D_\perp^2)^{1/2}$ to lower their energy.

Helicity and ferrotoroidic moment. We find that the spin textures smoothly evolve as a function of $D_\perp/D_\parallel$. The spiral continuously changes from a Bloch-like helix in the Dresselhaus limit to a Néel-like cycloid in the Rashba limit. In between, the spins tumble around an axis at an angle $\beta = \tan^{-1}(D_\perp/D_\parallel)$ to the $\mathbf{q}$ vector of the spiral. Similarly, the skyrmions smoothly evolve from vortexlike textures in the Dresselhaus limit to hedgehogs in the Rashba limit; see Fig. 1. In fact, $\gamma = \pi/2 - \beta$ is the "helicity" [3] of the skyrmions.

Our results imply that $D_\perp/D_\parallel$ controls the helicity γ, where Rashba $D_\perp$ could be tunable by electric field at an interface or by strain in a thin film. The ability to tune γ could be important in several ways. There is a recent proposal to use helicity to manipulate the Josephson effect in a superconductor/magnetic-skyrmion/superconductor junctions [26]. Another interesting phenomenon that depends on the helicity of skyrmions [27] is the "ferrotoroidic moment" $\mathbf{t} = (1/2)\int d^3r[\mathbf{r}\times\mathbf{m}(\mathbf{r})]$ [28,29]. We will show elsewhere that $\mathbf{t} = t_0\sin\gamma\,\hat{\mathbf{z}}$ for the SkX.

Rashba limit. Next, we turn to the $D_\parallel = 0$ results in the right panel of Fig. 1, where one has the maximum regime of the stability for the spiral and the hexagonal SkX, in addition to a small region with a square lattice SkX (first predicted in Ref. [30]), an elliptic cone phase, and a tilted FM. This phase diagram improves upon previous works [18,19,30]; see the Supplemental Material.

The tilted FM, which spontaneously breaks the $U(1)$ symmetry of $\mathcal{F}$ (in a field), has $m_z = H/2A$ and exists in the regime $2A > H$ and $AJ/D_\perp^2 > 2$ for $D_\parallel = 0$. We also see a new phase where the spins trace out a cone with an elliptic cross section. The elliptic cone axis makes an angle $\theta_0 = \cos^{-1}(H/2A)$ with $\hat{\mathbf{z}}$, and the spatial variation of $\mathbf{m}$ is along a $\mathbf{q}$ vector in the x-y plane.

In Fig. 1, thick lines denote continuous while thin lines denote first-order transitions; for details, see the Supplemental Material. $(A=2, H=4)J/D^2$ is a Lifshitz point [31] at which a state without broken symmetry (polarized FM) meets a

broken symmetry (tilted FM) and a modulated (elliptic cone) phase.

Let us next consider deviations from the pure Rashba limit to see how the extreme right panel of Fig. 1 evolves into the $D_\parallel \neq 0$ phase diagrams. As soon as one breaks bulk inversion, an infinitesimal $D_\parallel$ leads to the tilted FM being overwhelmed by the vertical cone, which gains Dresselhaus DM energy. On the other hand, the elliptic and vertical cone states compete for $D_\parallel \neq 0$ and for some small, but finite, $D_\parallel$ the vertical cone wins.

Spin textures and topological charge. There are interesting differences between the skyrmions for $H < 2A$ and $H > 2A$ ($H = 2A$ is marked as a dashed line in the phase diagrams of Fig. 1). For SkX with $H > 2A$, the focus of all the past work, the spins at the boundary of the unit cell (u.c.) are all up, parallel to the field. Hence one can make an isolated skyrmion [32] in a fully polarized FM background; see the leftmost panels of Fig. 2. The identification of the point at infinity in real space for an isolated skyrmion lets us define a map from $S^2 \to S^2$ and use the homotopy group $\pi_2(S^2) = \mathbb{Z}$ to characterize the topological charge or skyrmion number $N_{\rm sk}$.

In contrast, when $H < 2A$, the spins at the boundary are *not* all pointing up and the only constraint is periodic boundary conditions on the u.c.; see Fig. 2. There is no way to isolate this spin texture in a FM background. We must now consider the map $\mathbf{r} \to \mathbf{m}(\mathbf{r})$ from the u.c., which is a two-torus T^2 to S^2 in spin space (such maps are well known when T^2 represents a Brillouin zone in $\mathbf{k}$ space, but the mathematics is identical). This map is characterized by an integer Chern number $N_{\rm sk} = \int_{\rm u.c.} d^2\mathbf{r}\, \chi(\mathbf{r})$, where $\chi(\mathbf{r}) = \mathbf{m} \cdot (\partial_x \mathbf{m} \times \partial_y \mathbf{m})/4\pi$ is the topological charge density. In fact, one can use this definition of $N_{\rm sk}$ for all values of $H/2A$.

From the $A = 0$ panel on the left side of Fig. 2, we see that $\chi(\mathbf{r})$ is concentrated near the center of the u.c. and it is always of the same sign, as it is for all $H > 2A$. With increasing A, once $H < 2A$, we see that $\chi(\mathbf{r})$ begins to spread out and even changes sign within the u.c. In the square SkX phase χ is again concentrated, but this time in regions near the center and the edges of each u.c. along with regions of opposite sign at the u.c. corners. For $H \lesssim 2A$, the spin textures in the SkX phases are essentially composed of vortices and antivortices. Nevertheless, the Chern number argument shows that the total topological charge in each u.c. is an integer; $N_{\rm sk} = -1$ in all the panels of Fig. 2.

Discussion. Previous theories on understanding the increased stability on skyrmions in thin films of noncentrosymmetric materials [10,14–16] focused primarily on the changes in *uniaxial* magnetocrystalline anisotropy [13,33,34] with thickness, or on finite-size effects [35,36]. In fact, the latter can give rise to spin textures more complicated than skyrmion crystals, with variations in all three directions. However, none of these theories takes into account the role of broken surface inversion and Rashba SOC. As we have shown here, a nonzero Rashba $D_\perp$ leads to a greatly enhanced stability of the SkX phase, particularly for *easy-plane* anisotropy, while at the same time giving a handle on the helicity of skyrmions with an interesting internal structure.

We note that the phase diagrams in Fig. 1 apply to all systems with broken mirror symmetry, with or without bulk inversion. Mirror symmetry can be broken by certain crystal structures in bulk materials, by strain [24] in thin films, or by electric fields at the interfaces. For $D_\parallel = 0$ the vertical cone phase, which dominates much of the phase diagram for $D_\parallel \neq 0$, simply does not exist. Recently, we became aware of the observation [37] of hedgehoglike skyrmions in GaV_4S_8, a polar magnetic semiconductor with broken mirror symmetry, dominated by Rashba SOC. Skyrmions are, however, stabilized in this material only at finite temperature due to the large easy-axis anisotropy.

In conclusion, we have made a comprehensive study of the $T = 0$ phases of chiral magnets with two distinct DM terms. $D_\perp$ arises from Rashba SOC and broken surface inversion, while $D_\parallel$ comes from Dresselhaus SOC and broken bulk inversion symmetry. We predict that increasing the Rashba SOC and tuning magnetic anisotropy towards the easy-plane side will greatly help stabilize skyrmion phases. Our results are very general, based on a continuum "Ginzburg-Landau" energy functional whose form is dictated by symmetry. We hope that it will motivate *ab initio* density functional theory calculations of the relevant phenomenological parameters entering our theory and experimental investigations of skyrmions in Rashba systems.

Acknowledgments. We thank C. Batista, S. Lin, and Y. M. Lu for useful discussions. M.R. acknowledges support from NSF DMR-1410364. J.R. was supported by an NSF Graduate Research Fellowship, under Grant No. DGE-1343012, and by the CEM, an NSF MRSEC, under Grant No. DMR-1420451.

[1] A. Bogdanov and A. Hubert, J. Magn. Magn. Mater. **138**, 255 (1994).

[2] U. Rößler, A. Bogdanov, and C. Pfleiderer, Nature (London) **442**, 797 (2006).

[3] N. Nagaosa and Y. Tokura, Nat. Nanotechnol. **8**, 899 (2013).

[4] A. Neubauer, C. Pfleiderer, B. Binz, A. Rosch, R. Ritz, P. G. Niklowitz, and P. Böni, Phys. Rev. Lett. **102**, 186602 (2009).

[5] M. Lee, W. Kang, Y. Onose, Y. Tokura, and N. P. Ong, Phys. Rev. Lett. **102**, 186601 (2009).

[6] R. Ritz, M. Halder, M. Wagner, C. Franz, A. Bauer, and C. Pfleiderer, Nature (London) **497**, 231 (2013).

[7] N. Romming, C. Hanneken, M. Menzel, J. Bickel, B. Wolter, K. von Bergmann, A. Kubetzka, and R. Wiesendanger, Science **341**, 636 (2013).

[8] F. Jonietz, S. Mühlbauer, C. Pfleiderer, A. Neubauer, W. Münzer, A. Bauer, T. Adams, R. Georgii, P. Böni, R. Duine, K. Everschor, M. Garst, and A. Rosch, Science **330**, 1648 (2010).

[9] S. Mühlbauer, B. Binz, F. Jonietz, C. Pfleiderer, A. Rosch, A. Neubauer, R. Georgii, and P. Böni, Science **323**, 915 (2009).
[10] X. Yu, N. Kanazawa, Y. Onose, K. Kimoto, W. Zhang, S. Ishiwata, Y. Matsui, and Y. Tokura, Nat. Mater. **10**, 106 (2011).
[11] S. Seki, X. Yu, S. Ishiwata, and Y. Tokura, Science **336**, 198 (2012).
[12] B. Binz, A. Vishwanath, and V. Aji, Phys. Rev. Lett. **96**, 207202 (2006).
[13] M. N. Wilson, A. B. Butenko, A. N. Bogdanov, and T. L. Monchesky, Phys. Rev. B **89**, 094411 (2014).
[14] S. X. Huang and C. L. Chien, Phys. Rev. Lett. **108**, 267201 (2012).
[15] A. Tonomura, X. Yu, K. Yanagisawa, T. Matsuda, Y. Onose, N. Kanazawa, H. S. Park, and Y. Tokura, Nano Lett. **12**, 1673 (2012).
[16] X. Z. Yu, Y. Onose, N. Kanazawa, J. H. Park, J. H. Han, Y. Matsui, N. Nagaosa, and Y. Tokura, Nature (London) **465**, 901 (2010).
[17] S. Banerjee, O. Erten, and M. Randeria, Nat. Phys. **9**, 626 (2013).
[18] S. Banerjee, J. Rowland, O. Erten, and M. Randeria, Phys. Rev. X **4**, 031045 (2014).
[19] X. Li, W. V. Liu, and L. Balents, Phys. Rev. Lett. **112**, 067202 (2014).
[20] We note that this is adequate to describe long length scale textures, but not the atomic-scale skyrmions [38] that arise from competing local interactions.
[21] L. Shekhtman, O. Entin-Wohlman, and A. Aharony, Phys. Rev. Lett. **69**, 836 (1992).
[22] Y.-Q. Li, Y.-H. Liu, and Y. Zhou, Phys. Rev. B **84**, 205123 (2011).
[23] For films with thickness $\sim(J/D)a$, however, one may need other boundary conditions [35,36].
[24] Y. K. Kato, R. C. Myers, A. C. Gossard, and D. D. Awschalom, Science **306**, 1910 (2004).
[25] See Supplemental Material at http://link.aps.org/supplemental/10.1103/PhysRevB.93.020404 for further technical details.
[26] T. Yokoyama and J. Linder, Phys. Rev. B **92**, 060503 (2015).
[27] C. Batista (private communication).
[28] N. Spaldin, M. Fiebig, and M. Mostovoy, J. Phys.: Condens. Matter **20**, 434203 (2008).
[29] T. Castán, A. Planes, and A. Saxena, Phys. Rev. B **85**, 144429 (2012).
[30] S. Z. Lin, A. Saxena, and C. D. Batista, Phys. Rev. B **91**, 224407 (2015).
[31] P. M. Chaikin and T. C. Lubensky, *Principles of Condensed Matter Physics* (Cambridge University Press, Cambridge, UK, 1995).
[32] S.-Z. Lin, C. D. Batista, and A. Saxena, Phys. Rev. B **89**, 024415 (2014).
[33] M. N. Wilson, E. A. Karhu, A. S. Quigley, U. K. Rößler, A. B. Butenko, A. N. Bogdanov, M. D. Robertson, and T. L. Monchesky, Phys. Rev. B **86**, 144420 (2012).
[34] E. A. Karhu, U. K. Rößler, A. N. Bogdanov, S. Kahwaji, B. J. Kirby, H. Fritzsche, M. D. Robertson, C. F. Majkrzak, and T. L. Monchesky, Phys. Rev. B **85**, 094429 (2012).
[35] F. N. Rybakov, A. B. Borisov, and A. N. Bogdanov, Phys. Rev. B **87**, 094424 (2013).
[36] F. N. Rybakov, A. B. Borisov, S. Blügel, and N. S. Kiselev, Phys. Rev. Lett. **115**, 117201 (2015).
[37] I. Kézsmárki, S. Bordács, P. Milde, E. Neuber, L. M. Eng, J. S. White, H. M. Rønnow, C. D. Dewhurst, M. Mochizuki, K. Yanai, H. Nakamura, D. Ehlers, V. Tsurkan, and A. Loidl, Nat. Mater. **14**, 1116 (2015).
[38] S. Heinze, K. von Bergmann, M. Menzel, J. Brede, A. Kubetzka, R. Wiesendanger, G. Bihlmayer, and S. Blügel, Nat. Phys. **7**, 713 (2011).